Inorg. Chem. **2008**, *47*, 8704−8713

Synthesis and Characterization of Two Intensely Colored Tris(benzoylcyanoxime)iron(II) Anionic Complexes

Travis Owen,[†] Fernande Grandjean,[‡] Gary J. Long,*[,§] Konstantin V. Domasevitch,[⊥] and Nikolay Gerasimchuk*[,†]

Department of Chemistry, Temple Hall 431, Missouri State University, Springfield, Missouri 65897, Department of Physics, B5, University of Liège, B-4000 Sart-Tilman, Belgium, Department of Chemistry, Missouri University of Science and Technology, University of Missouri—Rolla, Rolla, Missouri 65409-0010, and Chemistry Department, Inorganic Chemistry Division, National University of the Ukraine, Volodimir'ska 64 St., Kiev 01033, Ukraine

Received March 8, 2008

Two intensely blue-colored complexes, $P(C_6H_5)_4[Fe(BCO)_3]$ (**1**) and $Na[Fe(BCO)_3]$ (**2**), where BCO^- is the benzoylcyanoxime anion, have been prepared and characterized in solution and in the solid state. The crystal structure of **1** has been determined at several temperatures (100, 155, 225, and 293 K) and consists of layers of $P(C_6H_5)_4^+$ cations and $[Fe(BCO)_3]^-$ anions. The latter exist as a pair of *fac*-Δ and Λ enantiomers in a monoclinic unit cell in the *P*2(1)/*n* space group. Iron(II) has a trigonal-prismatic N_3O_3 coordination environment with average Fe−N and Fe−O bond distances of 1.866 and 1.956 Å, respectively, bonds that are unusually short and indicate a $^1A_{1g}$ low-spin ground state for iron(II). A sample of **1** prepared with iron-57 has been studied by Mössbauer spectroscopy between 4.2 and 430 K and found to be low-spin iron(II) in studied temperature range. The stepwise formation constants for **1** in aqueous solution at 296 K and pH of 7 are $\log \beta_1 = 0.85 \pm 0.1$, $\log \beta_2 = 3.55 \pm 0.15$, and $\log \beta_3 = 6.36 \pm 0.15$. Both **1** and **2** exhibit irreversible oxidation of iron(II) at ~1.0 V, indicating a significant degree of the ligand-to-iron charge transfer. Thus, **1** and **2** are rare examples of highly colored iron(II) *anionic* complexes that do not contain aromatic heterocyclic amine ligands, such as bipyridine or phenanthroline.

Introduction

Intensely colored transition-metal complexes have numerous applications in various areas of chemistry, such as analytical, coordination, bioinorganic, medicinal, and physical chemistry. For example, some of these metal complexes are used for the spectrophotometric and fluorimetric determination of metal ions in solutions,[1] such as antitumor agents in photodynamic therapy,[2] cytotoxic intercalating compounds that affect DNA replication[3] and the cleavage of DNA,[4] and cell imaging materials.[5] In order to be useful in photodynamic therapy, colored complexes must possess water solubility and

* To whom correspondence should be addressed. E-mail: glong@mst.edu (G.J.L.), NNGerasimchuk@missouristate.edu (N.N.G.).
[†] Missouri State University.
[‡] University of Liège.
[§] University of Missouri—Rolla.
[⊥] National University of the Ukraine.

(1) (a) Burger, K. *Organic Reagents in Metal Analysis*; Pergamon, Oxford, U.K., 1973. (b) Sandell, E. B.; Hiroshi, O. *Photometric Determination of Traces of Metals*, 4th ed.; Wiley: New York, 1978. (c) Holtzbecher, Z. *Handbook of Organic Reagents in Inorganic Analysis*; Halsted Press: New York, 1976.

(2) (a) Bonnet, R. *Chemical Aspects of Photodynamic Therapy*; Gordon and Breach: London, 2000. (b) Rosenthal, D. I.; Nurenberg, P.; Becerra, C. R.; Frenkel, E. P.; Carbone, D. P.; Lum, B. L.; Miller, R.; Engel, J.; Young, S.; Miles, D.; Renschler, M. F. *Clin. Cancer Res.* **1999**, *5*, 739. (c) Woodburn, K.; Fan, Q.; Miles, D. *Photochem. Photobiol.* **1997**, *65*, 410. (d) Ali, H.; van Lier, J. E. *Chem. Rev.* **1999**, *99*, 2379.

(3) (a) Pyle, A. M.; Barton, J. K. In *Progress in Inorganic Chemistry*; Lippard, S. J., Ed.; John Wiley & Sons: New York, 1990; Vol. *38*, p 413. (b) Foxon, S. P.; Metcalfe, C.; Adams, H.; Webb, M.; Thomas, J. A. *Inorg. Chem.* **2007**, *46*, 409. (c) Tuite, E.; Lincoln, P.; Norden, B. *J. Am. Chem. Soc.* **1997**, *119*, 239. (d) Jenkins, Y.; Friedman, A. E.; Turro, N. J.; Barton, J. K. *Biochemistry* **1992**, *31*, 10809.

(4) (a) Armitage, B. *Chem. Rev.* **1998**, *98*, 1171. (b) Chifotides, H. T.; Dunbar, K. R. *Acc. Chem. Res.* **2005**, *38*, 146. (c) Erkkila, K. E.; Odom, D. T.; Barton, J. K. *Chem. Rev.* **1999**, *99*, 2777. (d) Szasiliwski, K.; Macyk, W.; Drzewiecka-Matuszek, A.; Brindell, M.; Stochel, G. *Chem. Rev.* **2005**, *105*, 2647. (e) Dhar, S.; Senapati, D.; Das, P. K.; Chattopadhyay, P.; Nethaji, M.; Chakravarty, A. R. *J. Am. Chem. Soc.* **2003**, *125*, 12118. (f) Janaratne, T. K.; Yadav, A.; Ongeri, F.; MacDonnel, F. M. *Inorg. Chem.* **2007**, *46*, 3420. (g) Deshpande, M. S.; Kumnbar, A. A.; Kumnbar, A. S. *Inorg. Chem.* **2007**, *46*, 5450.

10.1021/ic8004322 CCC: $40.75
Published on Web 09/04/2008

exhibit strong absorbance below > 600 nm. Photoactivation leads to a $^1\pi\pi^*$ state followed by the formation of the triplet $^3\pi\pi^*$ state that activates $^3O_2$ to the cytotoxic $^1O_2$ state through energy transfer. Recently, several iron-based metal complexes have been found to be efficient DNA photocleavage agents.[6] Further, intensely colored transition-metal complexes have been proposed for use in light-harvesting arrays,[7] nonlinear optical materials,[8] and the investigation of spin-crossover phenomena.[9] In the latter investigations, observed primarily in iron(II) complexes, a temperature-dependent spin equilibrium between the paramagnetic high-spin $^5T_{2g}$ state and the diamagnetic low-spin $^1A_{1g}$ state can be utilized in molecular electronics and data storage[10] or as molecular switches.[11] Spin transitions at close to room temperature observed, for example, in iron(II) pyrazolylborate complexes[12] make these complexes more attractive for practical considerations.

The vast majority of intensely colored transition-metal complexes have an octahedral or distorted octahedral coordination environment and are either neutral species or traditional cationic complexes with a $[M(L)_3]^{n+}$ composition, where *n* is 2 or 3, M is Ru, Co, Rh, Ir, or Fe, and L is dipyridine, phenanthroline, or one of their analogous, bipyrazine, terpyridine, or 2-picolylamine, bidentate ligands. The oxime-based boron-, tin(IV)-, or germanium(IV)-capped clathrochelate[13,14] "cages" also readily form neutral complexes with iron and cobalt. In contrast, little is known about intensely colored *anionic* iron(II) complexes with chelating ligands, although several $[FeL_3]^-$-type complexes have been reported.[15]

The above applications of intensely colored iron complexes in photobiology and materials science justify further investigation into their preparation and characterization. Because of their charge, anionic iron(II) complexes have an advantage for DNA binding because the base pairs in the latter have substantial partial positive charges. Herein, we present the results of the first part of a detailed study of two intensely colored blue anionic cyanoxime-based iron(II) complexes with the benzoylcyanoxime anion.[16−18]

Experimental Section

Materials and Methods. The HPLC-grade solvents used in the synthesis have been purchased from Aldrich and were deaerated under vacuum prior to use. Water was boiled under argon for 15 min and then cooled under bubbling argon. The organic solvents used for the spectroscopic measurements were all reagent grade and dried under fresh molecular sieves. High-purity $(NH_4)_2Fe(SO_4)_2\cdot 6H_2O$ was obtained from Fisher Scientific. Melting points and decomposition temperatures were determined under vacuum in closed capillary tubes with a Thomas-Hoover Uni-Melt apparatus. The C, H, N, and S elemental analyses were performed by the Atlantic Microlab, Norcross, GA.

Synthesis. The synthesis of benzoylcyanoxime ($C_9H_6N_2O_2$, HBCO) was carried out according to published procedures[16,17] from benzoylacetonitrile $[NCCH_2C(O)C_6H_5]$ obtained from Aldrich; see Scheme 1A. Benzoylcyanoxime is a pale-yellow waxy solid with a melting point of 119 °C. Its mass spectrum yielded a molecular mass of 174.0436 g/mol as compared with a calculated value for $C_9H_6N_2O_2$ of 174.0429 g/mol. IR spectrum (KBr), in cm^{-1}: 2232 ν(CN), 1655 ν(C═O), 1315 ν(CNO), 1060 ν(NO), 810 δ(CCNO). NMR spectra in DMSO-d_6: δ, in ppm, ^{1}H 15.12 (1H, oxime), 7.56 (1H, para), 7.72 (1H, meta), 7.91 (1H, ortho); $^{13}C\{^1H\}$ 108.7 (CN group), 185.4 (C═O), 135.2 (*ipso*-carbon), 134.2 (oxime carbon), 134.1, 128.9, 130.7 (CH).

The solid sodium salt of benzoylcyanoxime was not isolated and was used immediately after preparation to form its iron(II) complex. Its UV−visible spectrum in *n*-propanol exhibited the following transitions: λ_{max}, in nm (ϵ, in M^{-1} cm^{-1}) 251 (8900) $\pi \rightarrow \pi^*$ of the CN group; 309 (14200) $\pi \rightarrow \pi^*$; 457 (85) n $\rightarrow \pi^*$.

The preparation of the iron(II) complex salts of benzoylcyanoxime has been accomplished by using conventional techniques for the manipulation of air-sensitive compounds on a vacuum line or in Schlenkware.

(5) (a) Goldsmith, C. R.; Lippard, S. J. *Inorg. Chem.* **2006**, *45*, 555. (b) Mikata, Y.; Wakamatsu, M.; Kawamura, A.; Yamanaka, N.; Yano, S.; Odani, A.; Morihiro, K.; Tamotsu, S. *Inorg. Chem.* **2006**, *45*, 9262. (c) Holland, J. P.; Aigbirhio, F. I.; Betts, H. M.; Bonnitcha, P. D.; Burke, P.; Christlieb, M.; Churchill, G. C.; Cowley, A. R.; Dilworth, J. R.; Donnelly, P. S.; Green, J. C.; Peach, J. M.; Vasudevan, S. R.; Warren, J. E. *Inorg. Chem.* **2007**, *46*, 465.

(6) (a) Kraft, B. J.; Zaleski, J. M. *New J. Chem.* **2001**, *25*, 1281. (b) Roy, M.; Saha, S.; Patra, A. K.; Nethaji, M.; Chakravarty, A. R. *Inorg. Chem.* **2007**, *46*, 4368.

(7) (a) Bignozzi, C. A.; Argazzi, R.; Kleverlaan, C. J. *Chem. Soc. Rev.* **2000**, *29*, 87. (b) Fox, M. A., Chanon, M., Eds. *Photoinduced Electron Transfer*; Elsevier: Amsterdam, The Netherlands, 1988. (c) Gust, D.; Moore, T. A.; Moore, A. L. *J. Photochem. Photobiol. B* **2000**, *58*, 63. (d) Wojaczynski, J.; Latos-Grazynski, L. *Coord. Chem. Rev.* **2000**, *204*, 113. (e) Wagner, R. W.; Johnson, T. E.; Lindsey, J. S. *J. Am. Chem. Soc.* **1996**, *118*, 11166.

(8) (a) Norwood, R. A.; Sounik, J. R. *Appl. Phys. Lett.* **1992**, *60*, 295. (b) Ogawa, K.; Zhang, T.; Yoshihara, K.; Kobuke, Y. *J. Am. Chem. Soc.* **2002**, *124*, 22. (c) Kuebler, S. M.; Denning, R. G.; Anderson, H. L. *J. Am. Chem. Soc.* **2000**, *122*, 339–347.

(9) Gütlich, P., Goodwin, H. A., Eds. Spin Crossover in Transition Metal Compounds. Part I. *Topics in Current Chemistry*; Springer-Verlag: Berlin, 2004; Vol. *233*.

(10) Létard, J.-F.; Guionneau, P.; Goux-Capes, L. Spin Crossover in Transition Metal Compounds. Part III. *Topics in Current Chemistry*; Springer-Verlag: Berlin, 2004; Vol. *235*, pp 221−249.

(11) Reger, D. L.; Gardinier, J. R.; Elgin, J. D.; Smith, M. D.; Hautot, D.; Long, G. J.; Grandjean, F. *Inorg. Chem.* **2006**, 8862, and references cited therein.

(12) Long, G. J.; Grandjean, F.; Reger, D. L. Spin Crossover in Transition Metal Compounds. Part I . *Topics in Current Chemistry*; Springer-Verlag: Berlin, 2004; Vol. *233*, pp 91−122.

(13) (a) Geue, R. J.; Hambley, J. M.; Harrowfield, A. M.; Sargesson, A. M.; Snow, M. R. *J. Am. Chem. Soc.* **1984**, *106*, 5478–5488. (b) Martin, L. L.; Martin, R. L.; Murray, K. S.; Sargesson, A. M. *Inorg. Chem.* **1990**, *29*, 1387–1394. (c) Brown, K. N.; Geue, R. J.; Hambley, T. W.; Hockless, D. C. R.; Rae, A. D.; Sargesson, A. M. *Org. Biomol. Chem.* **2003**, *1*, 1598–15608. (d) Sargesson, A. M. *Coord. Chem. Rev.* **1996**, *151*, 89–114.

(14) (a) Voloshin, Y. Z.; Kostromina, N. A.; Kramer, R. *Clathrochelates: Synthesis, Structure and Properties*; Elsevier: Amsterdam, The Netherlands, 2002. (b) Voloshin, Y. Z.; Varzatskii, O. A.; Kron, T. E.; Bel'sky, V. K.; Zavodnik, V. E.; Pal'chik, A. V. *Inorg. Chem.* **2000**, *39*, 1907. (c) Voloshin, Y. Z.; Varzatskii, O. A.; Vorontsov, I. I.; Antipin, M. Y. *Angew. Chem., Int. Ed.* **2005**, *44*, 3400.

(15) (a) Gouzerh, P.; Jeannin, Y.; Miler-Srenger, E.; Valentini, F. *Acta Crystallogr., Sect. C* **1984**, *40*, 797. (b) Gouzerh, P.; Jeannin, Y.; Rocchiccioli-Deltcheff, C.; Valentini, F. *J. Coord. Chem.* **1979**, *9*, 221. (c) Raston, C. L.; White, A. H.; Golding, R. M. *J. Chem. Soc., Dalton Trans.* **1977**, 329.

(16) Ponomareva, V. V.; Dalley, N. K.; Kou, X.; Gerasimchuk, N. N.; Domasevitch, K. V. *J. Chem. Soc., Dalton Trans.* **1996**, 2351–2359.

(17) Gerasimchuk, N. N.; Skopenko, V. V.; Ponomareva, V. V.; Domasevitch, K. V. *Russ. J. Inorg. Chem.* **1993**, *38*, 964–970.

(18) Gerasimchuk, N. N.; Kuzmann, E.; Buki, A.; Vertes, A.; Nagy, L.; Burger, K. *Inorg. Chim. Acta* **1991**, *188*, 45–50.

Scheme 1

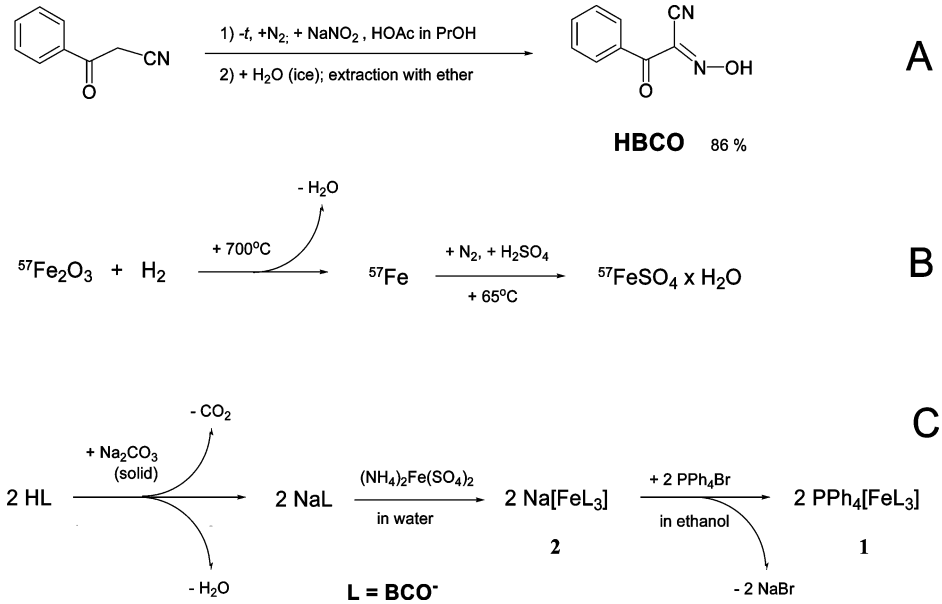

Preparation of $[P(C_6H_5)_4][Fe(BCO)_3]$ (1). The $[P(C_6H_5)_4]^+$ salt of benzoylcyanoxime may be prepared[19−22] in ethanol as the result of the metathesis reaction between Ag(BCO) and PPh_4Cl or PPh_4Br. In turn, the crimson Ag(BCO) salt quantitatively precipitates[17,18,24] upon mixing at room temperature equimolar concentrations of aqueous solutions of $AgNO_3$ and Na(BCO) or K(BCO).

Tetraphenylphosphonium tris(benzoylcyanoxime)iron(II), $[P(C_6H_5)_4][Fe(BCO)_3]$ (**1**), may be obtained either from a direct reaction between $P(C_6H_5)_4(BCO)$ and $(NH_4)_2Fe(SO_4)_2\cdot 6H_2O$ or by use of the dihydrate of $Na[Fe(BCO)_3]$ (**2**) as the precursor; see below and Scheme 1C; both methods lead to the practically quantitative preparation of the salt. Mixing, with stirring under argon, of 10 mL of an aqueous solution of 0.450 g (1.14 mM) of $(NH_4)_2Fe(SO_4)_2\cdot 6H_2O$ with 10 mL of an ethanol solution of 1.824 g (3.55 mM) of $P(C_6H_5)_4(BCO)$ generates a deep-blue-purple precipitate of **1**. The complex was filtered, washed with 10 mL of degassed water and 5 mL of cold methanol, and dried under vacuum; the yield was 0.99 g or 91%. Compound **1** was also obtained when a solution of **2** in water was added to a solution of $P(C_6H_5)_4Br$ in ethanol. When equal volumes of these solutions are used, no contamination of the precipitate of **1** with NaBr was observed. Anal. Calcd for $C_{51}H_{39}FeN_6O_8P$, $\mathbf{1}\cdot 2H_2O$: C, 64.43; H, 4.13; N, 8.84. Found: C, 62.67; H, 3.99; N, 8.64. Compound **1** can be dehydrated under 0.05 Torr vacuum at 65 °C in 24 h. IR spectrum (KBr), in cm^{-1}: 3100 ν(CH); 2220, 2215 ν(CN); 1635, 1627 ν(C═O); 1372 ν(CNO); 1238 ν(NO); 825 δ(CCNO). Complex **1** is soluble in most organic solvents and is insoluble in aliphatic hydrocarbons and water. Metallic iron-57 enriched to 94%, obtained from $^{57}Fe_2O_3$ by the reduction with hydrogen[23] at 700 °C and ambient pressure, was used to prepare $^{57}FeSO_4\cdot H_2O$; see Scheme 1. The latter was reacted with 3 equiv of Na(BCO) and then $P(C_6H_5)_4Br$ and resulted in the formation of **1** (Scheme 1).

Preparation of $Na[Fe(BCO)_3]$ (2). Sodium tris(benzoylcyanoxime)iron(II), $Na[Fe(BCO)_3]$ (**2**), was obtained upon mixing, with stirring under argon, 0.450 g (1.14 mM) of $(NH_4)_2Fe(SO_4)_2\cdot 6H_2O$ in 2 mL of deaerated water with 0.697 g (3.55 mM) of Na(BCO) in 10 mL of deaerated water. The reaction mixture immediately turned deep-blue, and a solid complex of the same color was formed. The amount of water was reduced to half under vacuum at 35 °C, and the precipitate of **2** was filtered, washed with 5 mL of degassed ice water, and dried under vacuum; the yield was 0.401 g or 59%, and the melting point of **2** is 220 °C. Anal. Calcd for $C_{27}H_{19}FeN_6NaO_8$, $\mathbf{2}\cdot 2H_2O$: C, 51.12; H, 3.02; N, 13.25. Found: C, 47.38; H, 3.04; N, 13.38. The compound may be dehydrated under 0.05 Torr vacuum at 65 °C in 8 h. IR spectrum (KBr), in cm^{-1}: 3120 ν(CH); 2230, 2225 ν(CN); 1630, 1620 ν(C═O); 1360 ν(CNO); 1235 ν(NO); 820 δ(CCNO). NMR spectra in CD_3OD: δ, in ppm, ^{1}H: 8.20 (doublet, 2H), 7.64 (triplet, 1H), 7.55 (triplet, 2H). Complex **2** is soluble in water and most organic solvents and is insoluble in aliphatic and aromatic hydrocarbons.

A photograph of **2** is shown in S4 in the Supporting Information. Both iron(II) complexes **1** and **2** are very air-stable as solids but in an air-exposed solution degrade over a period of weeks with a color change from deep-blue to reddish-brown.

Electrochemical Studies. The electrical conductivity of 0.001 M solutions of **1** and **2** in pure acetonitrile and water has been measured at 295 K with a YSI conductance-resistance meter model 34. Solutions of tetrabutylammonium bromide and tetraphenylphosphonium bromide, as 1:1 electrolytes, were used for electrode calibration.

The determination of the pK_a of HBCO was carried out with a Sirius Analytical Instruments Automated Titrimeter, Sussex, U.K., equipped with a temperature-controlled bath. Measurements consisted of a three-step multistage titration in water, with the ionic strength adjusted to 0.15 with KCl and the pH ranging from 3 to 11.

(19) Maher, T.; Gerasimchuk, N. N.; Durham, P.; Domasevitch, K. V.; Wilking, J.; Mokhir, A. *Inorg. Chem.* **2007**, *46*, 7268–7284.
(20) Arulsamy, N.; Bohle, S. D.; Doletski, B. G. *Inorg. Chem.* **1999**, *38*, 2709–2715.
(21) Domasevitch, K. V.; Gerasimchuk, N. N.; Mokhir, A. A. *Inorg. Chem.* **2000**, *39*, 1227–1237.
(22) Mokhir, A. A.; Gerasimchuk, N. N.; Pol'shin, E. V.; Domasevitch, K. V. *Russ. J. Inorg. Chem.* **1994**, *39*, 289–293.
(23) Brauer, G. *Handbuch der Präparativen Anorganischen Chemie*; Ferdinand Emke Verlag: Stuttgart, Germany, 1978; Chapter 5, section 1788.
(24) Skopenko, V. V.; Ponomareva, V. V.; Simonov, Yu. A.; Domasevitch, K. V.; Dvorkin, A. A. *Russ. J. Inorg. Chem.* **1994**, *39*, 1270–1277.
(25) (a) Sheldrick, G. M. *SADABS Area-Detector Absorption Correction*, version 2.03; University of Göttingen: Göttingen, Germany, 1999. (b) *SAINT: Data Integration Program*; Bruker AXS: Madison, WI, 1998.

Cyclic voltammetry measurements for **1** and **2** in dry degassed acetonitrile have been carried out at 296 K with a CH Instruments electrochemical analyzer, Austin, TX, equipped with a glassy carbon, 3-mm working electrode and a Ag/AgCl reference electrode obtained from Cypress Systems. The electrode was standardized with ferrocene in a CH_3CN solution containing 0.2 M LiClO; the Fc/Fc^+ couple exhibits a potential at $E_a = 0.31$ V versus a saturated calomel electrode. Iron complexes **1** and **2** were dissolved in pure CH_3CN containing 0.1 M $[N(C_4H_9)_4]PF_6$ and voltage sweeps were carried out over the range of ±1.2 V at a 50 mV/s scan rate.

Spectroscopic Studies. The UV−visible spectra of **1** and **2** and sodium benzoylcyanoxime have been recorded in solution at 296 K with a diode-array HP 8453 spectrophotometer over the range of 200−1100 nm using a freeze−thaw cycle with a 1-cm cuvette under anaerobic conditions; see S1 and S5 in the Supporting Information. A Bruker FTIR spectrometer was used for recording IR spectra over the range of 365−4000 cm^{-1}. A 400-MHz Varian Inova NMR spectrometer has been used to record, at ambient temperature, the ^1H and $^{13}C\{^1H\}$ spectra in CD_3OD and DMSO-d_6 with tetramethylsilane as an internal reference. Mass spectra of the organic ligands have been obtained with Autospec Q and ZAB spectrometers with a positive FAB, under argon and with *m*-nitrobenzylic alcohol as the matrix.

X-ray Structure Determination. The crystal structure of **1** has been determined at 100, 155, 225, and 293 K from a suitable prism-shaped crystal mounted on a plastic fiber. The low-temperature experiments were conducted using a Bruker AXS Kryoflex system with an accuracy of ±1 K. Diffraction measurements were made using a Bruker APEX2 instrument working in ω-scan mode and equipped with a SMART CCD area detector and with Mo Kα 0.710 73 Å radiation. Intensities were integrated from four series of 366 exposures, with each exposure covering 0.5° in ω and the total data set covering a sphere.[25b] The unit cell was determined at 155 K based on 197 reflections with $I \geq 20\sigma(I)$ from three series of 20 short (10 s) exposures. Numerical absorption corrections were applied based on indexed crystal faces obtained through video images of a crystal 360° rotation and by using Bruker AXS software[25a] (S13 in the Supporting Information). All structures were solved by direct methods using the *SHELX-97* program package and refined using the *SHELXTL-6.10* program by least squares on weighted F^2 values for all reflections.[26] All non-hydrogen atoms were refined with anisotropic displacement parameters and with no positional constraints. Because only 6 hydrogen atoms out of 35 were found on a difference map, the hydrogen atoms were attached to sp^2-hybridized carbon atoms of the phenyl groups optimized by a software C−H = 0.95 Å distance, and their positions were not further refined. Crystallographic data for **1** at 155 K are presented in Table 1, while data for all temperatures are compiled in S17 and S18 in the Supporting Information. Further details of the X-ray experiment can be found in the CIF file provided in the Supporting Information. PLATON reports on the structure determined at 155 K are listed in S2 and S3 in the Supporting Information. Figures describing the crystal structure of **1** were drawn using the Mercury and ORTEP 3 software packages.[27]

Mössbauer Spectroscopy. The Mössbauer spectra of **1** and **2** have been measured on a constant-acceleration spectrometer that utilized a room temperature rhodium matrix cobalt-57 source and was calibrated at room temperature with α-iron powder. The 4.2−295 K spectra of **1** and 85−295 K spectra of **2** have been measured in a standard Janis cryostat by using an absorber containing 3 mg/cm^2 of the iron-57-enriched sample of **1** and 50 mg/cm^2 of an unenriched sample of **2** mixed with boron nitride. The 295−430 K spectra of **1** have been measured in a high-vacuum water-cooled oven by using an absorber containing 8.5 mg/cm^2 of an iron-57-enriched sample of **1** mixed with boron nitride and pressed into a pellet at 1 g ton/cm^2 of pressure. There was no change in the sample upon heating to 430 K but continued heating to 450 K led to the irreversible decomposition of the absorber. The estimated relative errors are ±0.005 mm/s for the isomer shifts and quadrupole splittings, ±0.01 mm/s for the line widths, and ±0.003 (% ϵ)(mm/s) for the spectral absorption area. The absolute errors are approximately twice as large.

Table 1. Crystal Data and Structure Refinement for Tetraphenylphosphonium *fac*-Tris(benzoylcyanoximato)iron(II) $\{PPh_4[Fe(BCO)_3]$, **1**$\}$

parameter	
formula	$C_{51}H_{35}FeN_6O_6P$
mol wt, g/mol	914.67
color, shape	blue-purple prism
cryst size, mm	0.45 × 0.25 × 0.15
wavelength, Å	0.701 73
temperature, K	155(2)
density, Mg/m^3	1.38
cryst syst	monoclinic
space group	$P2(1)/n$ (No. 14)
unit cell, Å, deg	$a = 12.2043(12)$, $\alpha = 90.00$ $b = 25.991(3)$, $\beta = 92.4370(10)$ $c = 13.8507(13)$, $\gamma = 90.00$
volume, $Å^3$	4389.4(8)
abs coeff, mm^{-1}	0.439
$F(000)$	1888
θ range, deg	1.57−26.37
index ranges	$-15 < h < 15$, $-32 < k < 32$, $-17 < l < 17$
solution	direct methods
refinement method	full matrix least squares on F^2
reflns collected/unique	45003/9000
data/restrains/param	7255/0/586
GOF on F^2	1.020
final R indices $[I > 2\sigma(I)]$	0.0329 for 7255 $F_o > 4\sigma(F_o)$
R indices (all data)	0.0466 for all 9000 data
wR2	0.0759
wR2 (all data)	0.0837
largest diff peak/hole (e $Å^{-3}$)	0.37 and −0.37

Results and Discussion

Solution Spectroscopic Studies. Both the ^1H and $^{13}C\{^1H\}$ NMR spectra of **1** and **2** exhibit narrow sharp lines in the expected region for the organic moieties present (S6 in the Supporting Information). This observation indicates that **1** and **2** are, as expected, low-spin diamagnetic iron(II) complexes. No significant chemical shifts have been observed in the NMR spectra of the complexes as compared with either HBCO or its sodium salt.

The UV−visible spectra of complexes **1** and **2** exhibit a strong absorption at ~590 nm ($\epsilon > 13\,000\ M^{-1}\ cm^{-1}$), which is responsible for their intense deep-blue color; see Figure 1, Table 2, and S4 in the Supporting Information. This symmetric, single absorption band (S7 in the Supporting Information) results from a charge-transfer transition between the low-spin diamagnetic iron(II) and the cyanoxime ligand, a ligand that participates in π back bonding with the iron(II)

(26) XL: Crystal Structure Refinement. *SHELXTL*, version 6.10; Bruker AXS: Madison, WI, 2001.

(27) (a) Farrugia, L. *J. Appl. Crystallogr.* **1997**, *30*, 565. (b) Burnett, M. N.; Johnson, C. K. *ORTEP III*; Report ORNL-6895; Oak Ridge National Laboratory: Oak Ridge, TN, 1996.

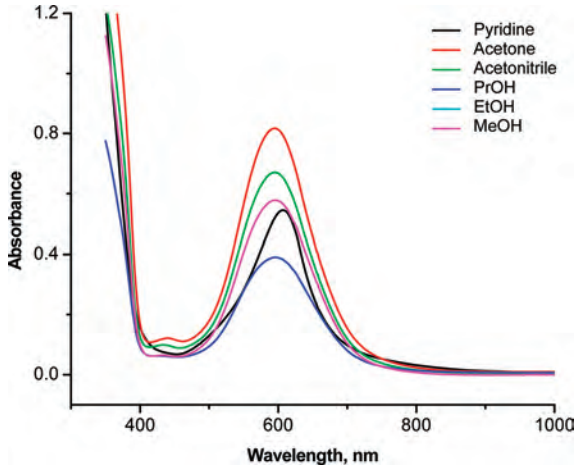

Figure 1. Room temperature visible spectra of **2** obtained in different solvents.

Table 2. Charge-Transfer Band in $[Fe(BCO)_3]^-$ at 293 K

solvent	λ_{max}, nm	ϵ, M^{-1} cm^{-1}
acetone	596	17 500
CH_3CN	594	18 000
CH_3OH	595	10 600
CH_3OH	596	15 000
i-C_3H_7OH	596	13 500
pyridine	607	14 000
DMF	595	13 300

ion through the nitrogen of the nitroso group.[28,29] The energy of this absorption band is solvent-dependent, which confirms its charge-transfer origin.[30] Previously studied red diamagnetic cationic iron(II) complexes exhibit significantly lower intensities of its charge-transfer bands, with the following parameters: $[Fe(dipy)_3]^{2+}$ (ϵ = 8700, at 522 nm), $[Fe(phen)_3]^{2+}$ (ϵ = 11 100 at 512 nm).[47] The values of the extinction coefficients, ϵ, of complexes **1** and **2** are very comparable with those of other intensely colored cationic coordination complexes that have successfully been used in photocytotoxicity and DNA binding studies. This similarity warrants an investigation of the interactions between complexes **1** and **2** and supercoiled DNA; the results of these photocleavage studies will be presented in a future publication.

Air-free solutions of **1** and **2** in organic solvents are very stable with time; however, these solutions are sensitive to both mineral and organic acids.

The formation constant of **2** has been determined in aqueous solution at 298 K by using a spectrophotometric method. The ionic strength was maintained constant at 0.01 with KCl, and a pH of 7 was maintained during all measurements in order to account for any protonation of BCO^- and hydrolysis of iron(II). The composition of the complexes formed between iron(II) and BCO^- was determined by Job's method and by stoichiometric dilution with a subsequent treatment of the results with Bjerrum's method; the principles of these calculations by the method of corresponding solutions can be extended to the treatment of results obtained by alternative methods.[31] According to the principles[32] governing hard and soft acid−base interactions, the octahedral tris complexes of iron(II) with an FeN_6 coordination environment are much more stable than similar iron(II) complexes with an FeN_3O_3 environment. In the latter case, a stepwise, consecutive complex formation is usually observed, and the tris complex becomes the predominant species only in an excess of the BCO^- ligand. This process can be written as

$$Fe^{2+} \xrightarrow{+BCO^-,\ \beta_1} [Fe(BCO)]^+ \xrightarrow{+BCO^-,\ \beta_2} [Fe(BCO)_2] \xrightarrow{+BCO^-,\ \beta_3} [Fe(BCO)_3]^- \quad (1)$$

The use of the Yatsimirskii method[33] yields formation constants of $\log \beta_1 = 0.85 \pm 0.1$, $\log \beta_2 = 3.55 \pm 0.15$, and $\log \beta_3 = 6.36 \pm 0.15$.

Electrochemistry. In spite of many papers devoted to the chemistry of benzoylcyanoxime HBCO,[16,17,34] its acidity in aqueous solutions has not been determined. The pK_a for this compound is found to be 3.53 ± 0.01, a value that indicates that HBCO is the strongest Brönsted acid of the 34 currently known cyanoximes.

Solution conductivity studies at 296 K of **1** and **2** indicate more than 50% dissociation in acetonitrile and the formation of 1:1 electrolytes in ethanol (S1 in the Supporting Information), which is consistent with the dissociations $Na[Fe(BCO)_3] \rightarrow Na^+ + [Fe(BCO)_3]^-$ and $[P(C_6H_5)_4][Fe(BCO)_3] \rightarrow [P(C_6H_5)_4]^+ + [Fe(BCO)_3]^-$. Some of the differences in the solution conductivity of **1** and **2** are due to differences in the mobility of the Na^+ and $[P(C_6H_5)_4]^+$ cations.

Cyclic voltammetry studies of **1** and **2** at 296 K (S8 in the Supporting Information) unexpectedly revealed a rather high irreversible iron(II) → iron(III) oxidation potential of ~1.0 V, a potential that indicates a significant degree of charge transfer from the cyanoxime ligand to iron(II) through π back bonding of the nitroso group. The surprising irreversibility of the redox process suggests the more thermodynamically preferable formation of *neutral* $Fe(BCO)_3$

(28) Gerasimchuk, N. N.; Nagy, L.; Schmidt, H.-G.; Noltemeyer, M.; Bohra, R.; Roesky, H. W. *Z. Naturforsch.* **1992**, *47b*, 1741–1745.
(29) (a) Chernov'yants, M. S.; Gus'kova, T. V.; Bagdasarov, K. N.; Nikitenko, I. A. *Zh. Anal. Khim.* **1984**, *39*, 798–800. (b) Bagdasarov, K. N.; Chernov'yants, M. S.; Tsupak, E. B.; Chernoivanova, T. M. 2-(Isonitrosocyanmethyl)benzimidazole Derivatives as Organic Reagents for Iron Determination. USSR Patent 19770228, 1977. (c) Bagdasarov, K. N.; Chernoivanova, T. M.; Chernov'yants, M. S. *Zavod. Lab.* **1983**, *49*, 4–5. (d) Knyazeva, T. V.; Gorbunova, M. O.; Chernaya, G. O. *Izv. Vyssh. Uchebn. Zaved., Pishch. Tekhnol.* **2000**, *2−3*, 90–92.
(30) (a) Reichardt, C. *Solvents and solvent effects in organic chemistry*, 3rd ed.; Wiley-VCH: New York, 2003; p 629, and references cited therein. (b) Kosower, E. M.; Hoffmann, D.; Wallenfels, K. *J. Am. Chem. Soc.* **1962**, *84*, 2755–2760. (c) Bakhsiev, N. G., Ed. *Sol'vatochromism: Problems and Methods*; Izdvo Leningradskogo Universiteta: Leningrad, 1989. (d) *Chem. Abstr.* **1990**, *112*, 186279g.
(31) Bjerrum, J. *Metal Ammine Complexes Formation in Aqueous Solutions*; Inorst. Lit.: Moscow, 1961.
(32) (a) Pearson, R. G., Ed.; *Hard and Soft Acids and Bases*; Dowden Hutchinson and Ross, Inc.: Stroudsburg, PA, 1973. (b) Miessler, G. L.; Tarr, D. A. *Inorganic Chemistry*, 2nd ed.; Prentice Hall: Upper Saddle River, NJ, 2000.
(33) Yatsimirskii, K. B.; Milyukov, P. M. *Zh. Fiz. Khim.* **1957**, *31*, 842–850.
(34) (a) Ponomareva, V. V.; Skopenko, V. V.; Domasevitch, K. V.; Sieler, J.; Gelbrich, T. *Z. Natuforsch.* **1997**, *52b*, 901–905. (b) Domasevitch, K. V.; Ponomareva, V. V.; Rusanov, E. B. *J. Coord. Chem.* **1995**, *34*, 259–263.

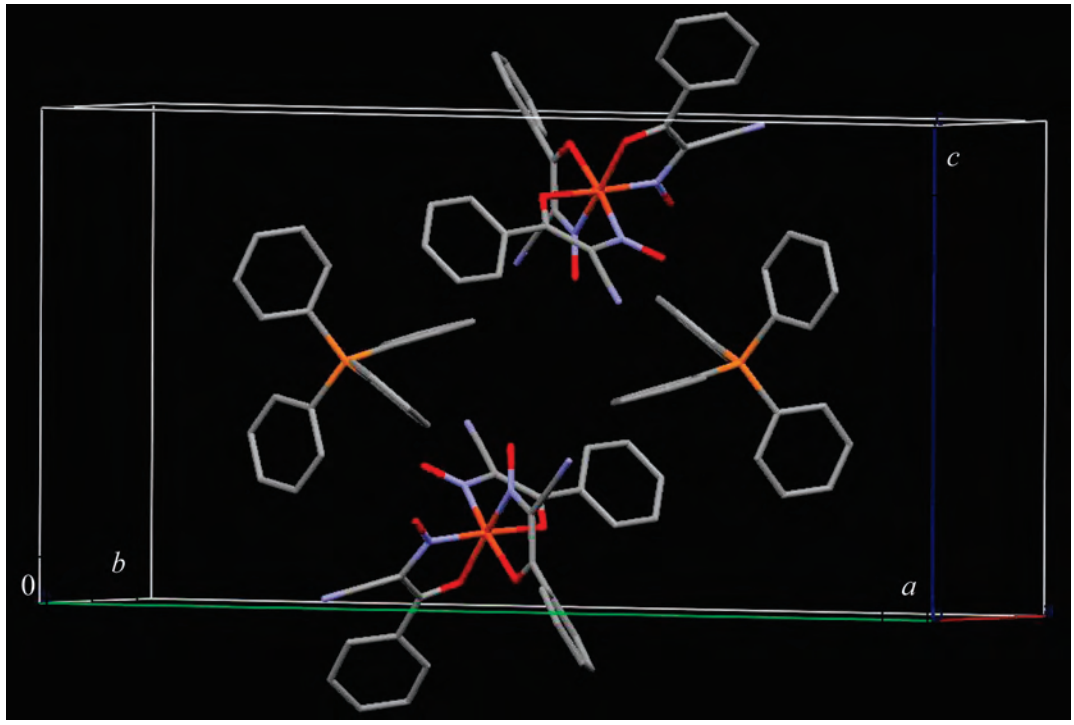

Figure 2. Portion of the unit cell of **1** showing an enantiomeric pair of the anions (only two out of four molecules of the complex are displayed). Color scheme: blue, nitrogen; red, oxygen; orange, phosphorus; gray, carbon. The hydrogen atoms have been omitted for clarity.

complex, species that become resistant to reduction back to the *anionic* $[Fe(BCO)_3]^-$ complexes.

X-ray Structural Results. A single crystal suitable for the determination of the structure of **1** was obtained from the mother liquor remaining after the initial precipitation. Complex **1**, which has an island-type structure consisting of the large phosphonium cations and large tris(cyanoximato)iron(II) anions (see Figure 2), crystallizes as the *fac*-isomer with two optical isomers Δ and Λ; because of the monoclinic centrosymmetric *P*2(1)/*n* space group, two enantiomeric pairs of **1** are found in one unit cell. The cyanoxime anion in the complex forms five-membered chelate rings; the structure of the Δ-*fac* isomer of the $[Fe(BCO)_3]^-$ anion and the atomic numbering scheme are shown in Figure 3. The coordination environment of the low-spin iron(II) is a distorted trigonal antiprism; see Figure 4.

Complex **1** is a rare case of a mixed-donor FeN_3O_3 coordination environment with three very short Fe−N bond lengths of 1.8716(14), 1.8634(14), and 1.8615(14) Å. Similarly, there are three short Fe−O bonds of 1.9477(12), 1.9596(12), and 1.9602(12) Å. Both the Fe−N and Fe−O bond lengths are significantly shorter than the 2.45 and 2.06 Å sum of their respective ionic radii,[50] a shortening that indicates the considerable covalent character of these bonds; see Table 3. More specifically, this coordination environment produces a strong ligand field and thus a low-spin $^1A_{1g}$ electronic ground state for the iron(II) ion. Geometrical parameters for identical Δ- and Λ-$[Fe(BCO)_3]^-$ anions in **1** are summarized in Table 3. The structure of the tetraphenylphosphonium cation is completely normal and is not discussed in detail herein. All of the cyanoxime anions, which

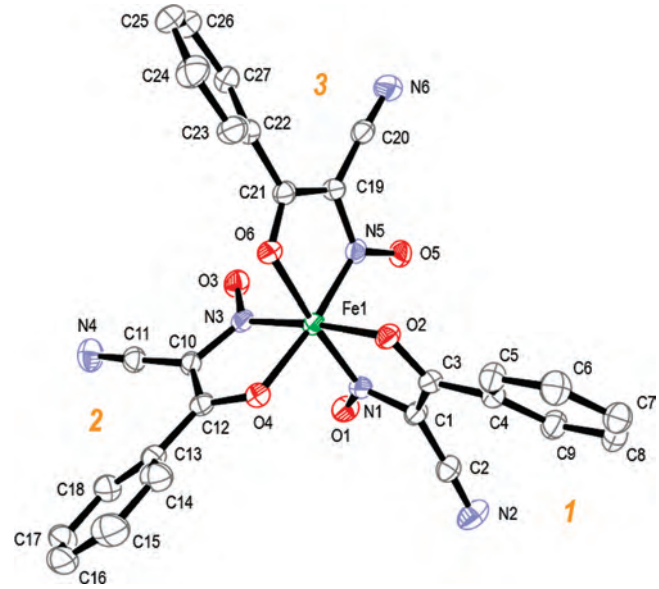

Figure 3. Numbering scheme and molecular structure of the Δ-*fac*-$[Fe(BCO)_3]^-$ anion of **1** at 155 K. The numbers of the three different bidentate cyanoxime ligands are indicated in orange. The hydrogen atoms have been omitted for clarity, and the figure is drawn with 50% probability ellipsoids.

adopt the trans-anti configuration[35] in **1**, are in the nitroso form, as is evident from the much shorter N−O than C−N bond lengths; see Table 3. Indeed, the average N−O bond distance in **1** is 1.252 Å, a distance that is practically the same as the classic N=O double bond distance of 1.22 ± 0.02 Å found in organic nitrites.[36] The three nonplanar BCO^- anions in **1** are crystallographically distinct (see Table 3),

(35) Robertson, D.; Cannon, J.; Gerasimchuk, N. N. *Inorg. Chem.* **2005**, *44*, 8326–8342.

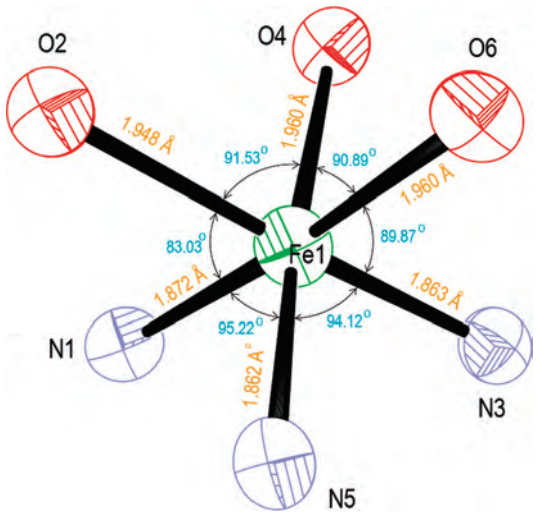

Figure 4. Trigonal-antiprismatic geometry of the coordination polyhedron in the structure of **1** at 155 K.

Table 3. Selected Bond Lengths and Angles in **1** at 155 K[a]

bond length, Å		angle, deg	
O1−N1	1.2528(2)	N1−C1−C3	112.90(14)
O2−C3	1.2703(19)	N1−C1−C2	119.93(15)
O3−N3	1.2514(18)	C3−C1−C2	127.02(15)
O4−C12	1.269(2)	N2−C2−C1	177.1(2)
O5−N5	1.2522(18)	O2−C3−C1	116.69(15)
O6−C21	1.270(2)	O2−C3−C4	118.29(15)
N1−C1	1.376(2)	C1−C3−C4	125.02(15)
N2−C2	1.148(2)	N3−C10−C12	112.87(15)
N3−C10	1.384(2)	N3−C10−C11	118.48(15)
N4−C11	1.141(2)	C12−C10−C11	128.52(16)
N5−C19	1.380(2)	N4−C11−C10	178.7(2)
N6−C20	1.145(2)	O4−C12−C10	116.55(15)
C1−C3	1.421(2)	O4−C12−C13	118.36(15)
C1−C2	1.420(2)	C10−C12−C13	125.08(16)
C3−C4	1.475(2)	N5−C19−C20	119.27(15)
C10−C12	1.417(2)	N5−C19−C21	112.90(15)
C10−C11	1.426(2)	C20−C19−C21	127.62(16)
C12−C13	1.475(2)	N6−C20−C19	177.10(19)
C19−C20	1.422(2)	O6−C21−C19	117.09(15)
C19−C21	1.417(2)	O6−C21−C22	118.44(15)
C21−C22	1.478(2)	C19−C21−C22	124.47(15)
		O1−N1−C1	119.22(14)
		O3−N3−C10	118.32(14)
		O5−N5−C19	119.07(14)
		N1−Fe1−N3	95.51(6)
		N1−Fe1−O6	174.48(6)
		N5−Fe1−O6	83.16(6)
		N3−Fe1−O2	173.98(6)
		N5−Fe1−O2	91.84(5)
		O6−Fe1−O2	91.73(5)
		N1−Fe1−O4	91.00(6)
		N3−Fe1−O4	82.64(6)
		N5−Fe1−O4	173.25(5)
		C3−O2−Fe1	113.43(11)
		C12−O4−Fe1	113.63(11)
		C21−O6−Fe1	112.50(11)
		O1−N1−Fe1	126.96(11)
		C1−N1−Fe1	113.71(11)
		O3−N3−Fe1	127.33(11)
		C10−N3−Fe1	114.26(11)
		O5−N5−Fe1	127.19(11)
		C19−N5−Fe1	113.75(11)

[a] Bond lengths and angles for the Fe−N and Fe−O bonds are shown in Figure 4.

but, nevertheless, they have the common feature of conjugated nitroso and carbonyl groups that form tight, planar, five-membered chelation rings; see Figure 3. More specifically, the chelating BCO^- ligand 1 has C1−N1−Fe1−O2 and C3−O2−Fe1−N1 torsion angles of +4.10° and −1.84°, respectively, whereas the planar core has O1−N1−C1−C3 and N1−C1−C3−O2 torsion angles of 178.06° and 4.16°, respectively. The analogous angles for ligand 2 are +1.77° and −1.01° and −179.01° and +1.40°; this ligand displays the least deviation from planarity. Finally, the analogous angles for BCO^- ligand 3 are −5.96° and +7.20° and 175.49° and 2.17°. The average chelating "bite angle" N−Fe1−O in the structure is 82.94°. The phenyl groups are out of the plane of the conjugated oxime carbonyl groups, with torsion angles ranging from 21.75° for ligand 1, to 25.14° for ligand 2, and to 39.07° for ligand 3. The cyano groups in all three of the BCO^- anions in **1** are linear but are also out of the plane of the conjugated core of the ligand, with torsion angles ranging from 15° to 26°. Molecules of **1** form alternating layers of $[Fe(BCO)_3]^-$ anions and $[P(C_6H_5)_4]^+$ cations; the anion−cation packing diagram is shown in S9 in the Supporting Information. The temperature dependence of the crystal structure of **1** is summarized in S14−S16 in the Supporting Information. The unit cell parameters increase and the density decreases as expected upon warming. In contrast, the iron(II) bond lengths do not increase significantly upon warming, but the torsion angles of the phenyl groups in both the $[Fe(BCO)_3]^-$ anion and the PPh_4^+ cation increase upon warming. These torsion angle increases of only a few degrees permit the phenyl groups to adopt a more compact conformation, which is reflected in the increased density of **1** at low temperatures even in the absence of any significant shortening of the iron(II) bonds. However, in agreement with the Mössbauer spectral results presented below, the isotropic thermal parameter, U_{iso}, for the iron(II) ion increases linearly with temperature; see S16 in the Supporting Information.

A search of the Cambridge structural database for iron(II) complexes with the FeN_3O_3 mixed-donor coordination polyhedra with Fe−N bond distances of 1.86 Å or less and Fe−O bond distances of 1.95 Å or less yielded 96 complexes. Of these 96 complexes, only 17 had five-membered iron(II) chelation rings, and of these 17 complexes, only 5 had iron(II) bonds shorter than both 1.86 Å for Fe−N and 1.95 Å for Fe−O; see S10−S12 in the Supporting Information. Among those five complexes, three were formed with the same FeL_3^- anion and the tetraphenylarsonium, tetraphenylphosphonium,[15a] and cesium[15b] cations. In all three of these complexes, there are also different Fe−N and Fe−O bonds. A comparison of the sums of the averaged Fe−O and Fe−N bond distances, D_{ave}, revealed different degrees of binding "tightness" at the iron(II) ion. On the basis of this criterion, i.e., $D_{ave} = D_{Fe-O,\ ave} + D_{Fe-N,\ ave}$, complex **1**, with D_{ave} = 1.957 Å + 1.868 Å = 3.825 Å, has one of the shortest D_{ave} values and, thus, is one of a very small number of low-spin iron(II) complexes with the FeN_3O_3 mixed-donor coordination environment.

(36) Gordon, A. J.; Ford, R. A. *The Chemist Companion (Handbook)*; John Wiley & Sons: New York, 1972.

Table 4. Mössbauer Spectral Parameters

complex	T, K	δ,[a] mm/s	ΔE_Q, mm/s	Γ, mm/s	area, (% ϵ)(mm/s)
$[P(C_6H_5)_4][Fe(BCO)_3]$ (**1**)	430	0.1065	0.408	0.29	1.314
	410	0.1205	0.416	0.28	1.530
	390	0.1275	0.426	0.28	1.706
	370	0.1385	0.431	0.31	2.081
	350	0.1505	0.439	0.31	2.402
	310	0.1675	0.455	0.30	3.219
	295	0.174	0.459	0.30	3.563
	225	0.201	0.476	0.31	5.775
	155	0.225	0.490	0.32	8.813
	85	0.240	0.495	0.32	11.80
	45	0.241	0.502	0.33	15.36
	25	0.242	0.507	0.33	16.30
	4.2	0.241	0.503	0.33	16.79
$Na[Fe(BCO)_3]$ (**2**)	295	0.214	0.536	0.36	1.225
	250	0.222	0.577	0.31	2.016
	225	0.233	0.574	0.30	1.835
	200	0.230	0.585	0.30	3.646
	155	0.250	0.598	0.28	5.807
	85	0.255	0.606	0.29	8.154
	60	0.254	0.615	0.27	9.013
	40	0.254	0.619	0.27	9.881
	20	0.256	0.615	0.28	10.79
	4.2	0.257	0.619	0.27	11.34

[a] The isomer shifts are given relative to α-iron powder at room temperature.

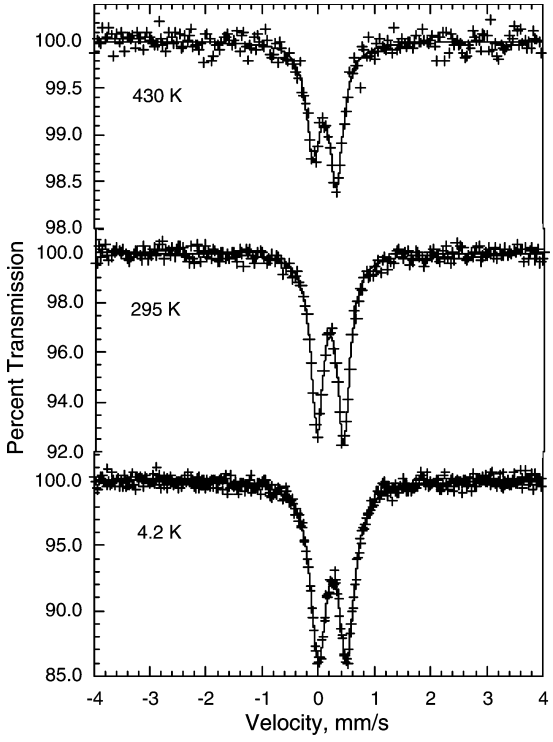

Figure 5. Iron-57 Mössbauer spectra of **1** obtained at 4.2, 295, and 430 K.

Mössbauer Spectral Results. The Mössbauer spectra of **1**, obtained between 4.2 and 430 K, and of **2**, obtained between 4.2 and 295 K, have been fit with a single quadrupole doublet with a single line width but with slightly different areas for the two components of the doublet spectra of **1**; the resulting parameters are given in Table 4, and representative spectra of **1** are shown in Figure 5. The spectra of **2** are very similar to those shown in Figure 5. The hyperfine parameters of **1** and **2** are fully consistent with the presence of low-spin iron(II) in a somewhat distorted coordination environment. The small asymmetry in the areas of the doublet lines of **1** results from a small amount of texture in the absorber, texture that is more apparent in the 295−430 K spectra because this absorber had to be compressed into a boron nitride pellet to remain intact in the oven.

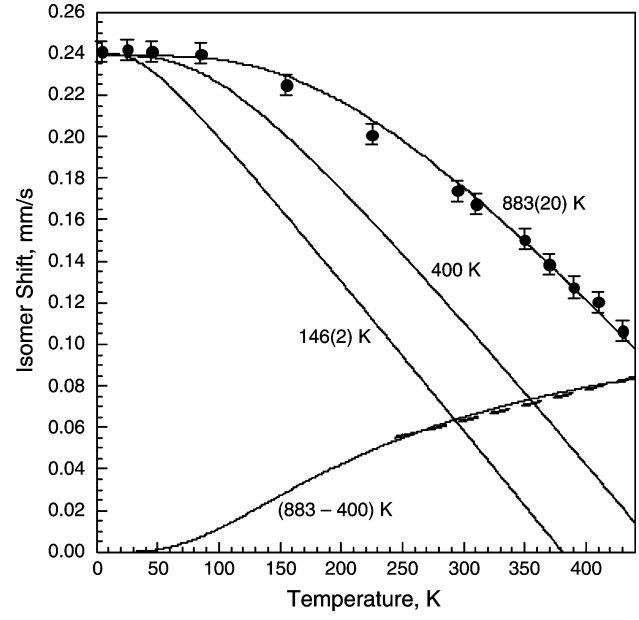

Figure 6. Temperature dependence of the isomer shift of **1** fit with the Debye model for a solid. The remaining lines are discussed in the text.

The temperature dependences of the isomer shift of **1** (see Figure 6) and **2** are well fit with the Debye model[37] for the second-order Doppler shift with characteristic Mössbauer temperatures, Θ_M^{δ}, of 883(20) and 1066(51) K, respectively. These temperatures are much larger than the Mössbauer temperatures, Θ_M^{A}, of 146(2) and 128(4) K obtained from the temperature dependence of the logarithm of the spectral absorption area; see Figure 7. However, as shown in this

(37) Shenoy, G. K.; Wagner, F. E.; Kalvius, G. M. In *Mössbauer Isomer Shifts*; Shenoy, G. K., Wagner, F. E., Eds.; North-Holland: Amsterdam, The Netherlands, 1978; p 49.

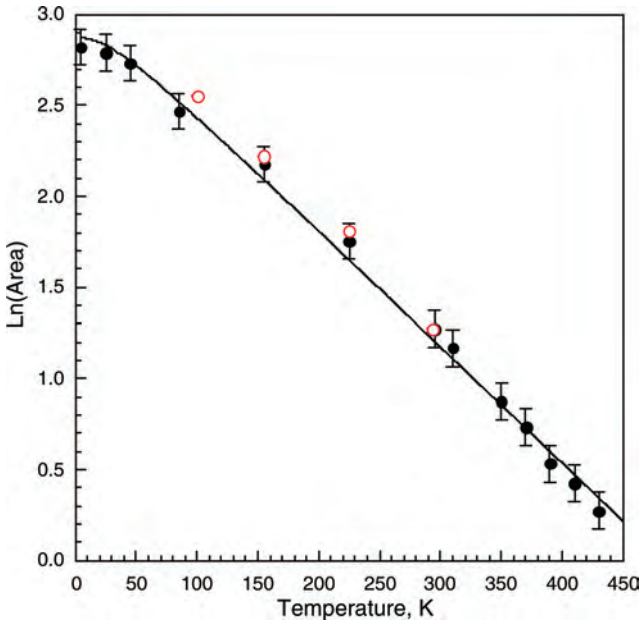

Figure 7. Temperature dependence of the logarithm of the spectral absorption area, the black points, of **1** fit with the Debye model for a solid. The corresponding logarithm of the iron(II) anisotropic thermal parameters, U_{iso}, normalized at 293 K, are shown in red for comparison.

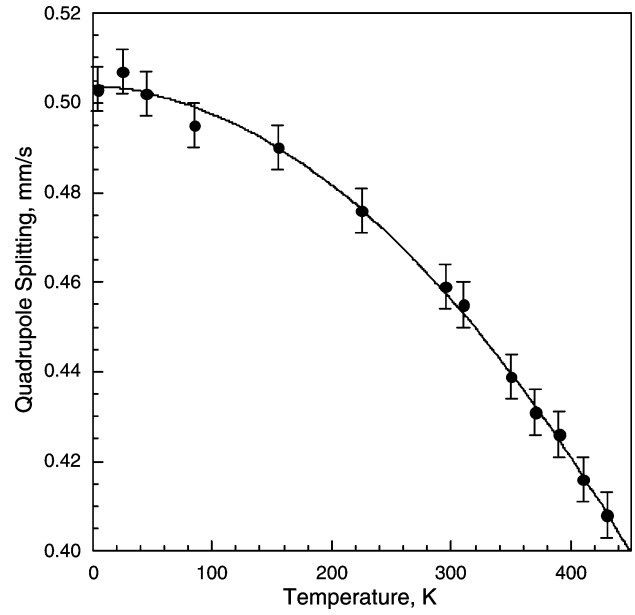

Figure 8. Temperature dependence of the quadrupole splitting of **1**.

figure, there is excellent agreement between the temperature dependence of the logarithm of the spectral absorption area and the iron(II) isotropic thermal parameter, U_{iso}.

It is well-known[37,48,49] that the two Mössbauer temperatures, $\Theta_M{}^{\delta}$ and $\Theta_M{}^{A}$, obtained from the two temperature dependences are usually different because they depend, for the isomer shift, on $\langle v^2 \rangle$, the mean-square vibrational velocity of the iron-57, and, for the absorption area, on $\langle x^2 \rangle$, the mean-square atomic displacement of the iron-57; there is no model-independent relationship between these mean square values.[37] However, measurements of the Mössbauer temperatures on related iron(II) complexes[38,39] indicate that $\Theta_M{}^{\delta}$ is often at least twice as large as $\Theta_M{}^{A}$ and is as much as 5 times larger for some nitroprusside salts. This difference is especially pronounced for low-spin iron(II) complexes[48,49] because, for the isomer shift, the difference depends on $\langle v^2 \rangle$, a velocity that is mostly dependent upon molecular vibrations in the range of 400−800 cm^{-1}, whereas for the spectral absorption area, it depends on $\langle x^2 \rangle$, a displacement that is strongly affected by lattice vibrations found at 250 cm^{-1} or below. In **2**, the ν(Fe−O) and ν(Fe−N) vibrational bands were observed at 588 and 816 cm^{-1}, respectively. The isomer shift of **1** (see Figure 6) decreases by only 0.135 mm/s between 4.2 and 430 K, or far less than would be expected on the basis of the 146(2) K value of $\Theta_M{}^{A}$. Thus, we have calculated the temperature dependence of the isomer shift expected on the basis of the second-order Doppler shift for a $\Theta_M{}^{\delta}$ of 400 K, a reasonable value in view of the 146(2) K value of $\Theta_M{}^{A}$; see Figure 6. The positive difference between this calculated temperature dependence and the observed temperature dependence is shown in Figure 6 as the line labeled "(883−400) K", and the difference is assumed to result from the influence of the lattice expansion on the isomer shift. As the lattice expands with increasing temperature, the electron density at the iron nucleus decreases and the isomer shift increases. The linear fit between 250 and 430 K, shown as the thicker broken line, yields a lattice expansion[40] of the isomer shift of 1.49×10^{-4} (mm/s)/K.

The temperature dependence of the quadrupole splitting of **1** is shown in Figure 8; the results for **2** are very similar. In a low-spin iron(II) compound, there are two contributions to the electric field gradient at the iron nucleus, the lattice and covalency contributions.[41] Neither of these contributions is known to show an extensive temperature dependence. Hence, the decrease in the quadrupole splitting by 0.095 mm/s or 19% between 4.2 and 430 K is surprising. The fit of the temperature dependence for **1** shown in Figure 8 corresponds to a quadratic dependence,[42,43]

$$\Delta E_Q(T) = \Delta E_Q(0)\,[1 - aT - bT^2]$$

with $\Delta E_Q(0) = 0.504$ mm/s, $a = 2.86 \times 10^{-5}$ (mm/s)/K^{-1}, and $b = 9.58 \times 10^{-7}$ (mm/s)/K^{-2}. The corresponding values for **2** are $\Delta E_Q(0) = 0.616$ mm/s, $a = 3.88 \times 10^{-5}$ (mm/s)/K^{-1}, and $b = 9.73 \times 10^{-7}$ (mm/s)/K^{-2}. Such a quadratic dependence has been observed[42,43] in metallic compounds, but it is empirical and is not supported by any adequate theoretical model. In $ZnFe_2O_4$ and $CdFe_2O_4$, the quadrupole splitting at iron(III) results only from a lattice contribution

(38) (a) Reger, D. L.; Elgin, J. D.; Smith, M. D.; Grandjean, F.; Rebbouh, L.; Long, G. J. *Polyhedron* **2006**, *25*, 2616. (b) Reger, D. L.; Gardinier, J. R.; Bakbak, S.; Gemmill, W.; Smith, M. D.; Rebbouh, L.; Grandjean, F.; Shahin, A. M.; Long, G. J. *J. Am. Chem. Soc.* **2005**, *127*, 2303. (c) Reger, D. L.; Gardinier, J. R.; Smith, M. D.; Shahin, A. M.; Long, G. J.; Rebbouh, L.; Grandjean, F. *Inorg. Chem.* **2005**, *44*, 1852.
(39) Jiao, J.; Long, G. J.; Rebbouh, L.; Grandjean, F.; Beatty, A. M.; Fehlner, T. P. *J. Am. Chem. Soc.* **2005**, *127*, 17819.
(40) Ingalls, R.; Van der Woude, F.; Sawatzky, G. A. In *Mössbauer Isomer Shifts*; Shenoy, G. K., Wagner, F. E., Eds.; North-Holland: Amsterdam, The Netherlands, 1978; p 361.
(41) Golding, R. M. *Mol. Phys.* **1967**, *12*, 13.
(42) Varma, C.; Rao, G. N. *Hyperfine Interact.* **1983**, *16*, 207.
(43) Vianden, R. *Hyperfine Interact.* **1983**, *16*, 189.

and decreases[44,45] linearly with temperature with slopes of 4×10^{-5} and 3.2×10^{-5} (mm/s)/K, respectively. These decreases are too large to result only from the thermal expansion of the lattice and have been attributed to a reduction in the symmetry of the local coordination environment with increasing temperature. The temperature dependence of the quadrupole splitting in a low-spin iron(II) compound has been found[46] to be linear with a slope of -3.5×10^{-5} (mm/s)/K. Hence, the temperature dependence of the quadrupole splitting observed herein is much steeper than all previously reported temperature dependences of the quadrupole splitting in low-spin iron(II) and iron(III) compounds. In order to explain the substantial increase in the quadrupole splitting with decreasing temperature, we propose the following. From the X-ray diffraction measurements between 100 and 293 K, we know that the Fe−N and Fe−O bond distances are very short and virtually unchanged. However, as the temperature decreases, the torsion angles of the phenyl group change and most likely induce a change in distortion that increases the electric field gradient at iron(II) and, thus, the lattice contribution to the quadrupole splitting.

Conclusions

This work is the first part of the project whose objective is to obtain highly colored anionic iron(II) complexes for subsequent studies of their interactions with DNA. Thus, anionic tris(benzoylcyanoximato)iron(II) salts of Na^+ and $P(C_6H_5)_4^+$ were obtained in high yield from Fe^{2+} inorganic precursors and triple excess of the deprotonated cyanoxime ligand. The stepwise formation constants of the $[Fe(BCO)_3]^-$ complex anion were measured in aqueous solutions at neutral pH and evidenced great stability ($\log \beta_3 = 6.36$) of the compound. Both Na^+ and $P(C_6H_5)_4^+$ complexes have an intense blue color due to a single charge-transfer band at ~596 nm with $\epsilon > 13\,000\ M^{-1}\ cm^{-1}$, with the central atom of iron(II) in both compounds being in the low-spin $^1A_{1g}$ state. $Na[Fe(BCO)_3]$ is soluble in most organic solvents and water. This fact, together with the complex stability in aqueous solutions, makes this compound very attractive for DNA binding studies, the results of which will be reported in a forthcoming publication.

Acknowledgment. The authors appreciate the help of both David Vinyard of Missouri State University in obtaining the electrochemical measurements and Dr. Moulay T. Sougrati in obtaining some of the Mössbauer spectra and Dr. Svitlana Silchenko, of Absorption Systems, for the ligand acidity constant measurements. The authors acknowledge, with thanks, the ACS Petroleum Research Fund for financial support received through Grant 39079-B3, the Fonds National de la Recherche Scientifique, Belgium, for financial support received through Grants 9.456595 and 1.5.064.05, and Missouri State University for a faculty research grant (NG).

Supporting Information Available: The results of electrical conductivity measurements of solutions of **1** and **2** (S1); PLATON reports on the crystal structure of **1** (S2 and S3); a photograph of the deep-blue complex, **2** (S4); the design of a quartz 1-cm cuvette for air-free UV−visible spectroscopic measurements (S5); the ^1H NMR spectrum of **2** obtained in CD_3OD (S6); the deconvolution of the UV−vis spectrum of **2** in DMF (S7); the cyclic voltammetry curve of **2** (S8); the crystal packing observed for **1** (S9); fragments of the structures of iron(II) complexes found in CSDB with unusually short Fe−N and Fe−O bonds (S10−S12); indexed crystal faces (S13); effects of temperature on the cell constants and Fe−ligand bond lengths (S14), on the torsion angles in the phenyl group of cyanoxime anions (S15), and on the U_{iso} parameter of the Fe atom in the structure of **1** (S16); crystal and refinement data for **1** at studied temperatures (S17 and S18); and CIF files for the structure of **1** at different temperatures. This material is available free of charge via the Internet at http://pubs.asc.org.

IC8004322

(44) Vandenberghe, R.; DeGrave, E. In *Mössbauer Spectroscopy Applied to Inorganic Chemistry*; Long, G. J., Grandjean, F., Eds.; Plenum Press: New York, 1989; Vol. *3*, p 59.
(45) Karner, W.; Wäppling, R.; Nagarajan, T. *Phys. Scr.* **1987**, *36*, 544.
(46) Silva, R. M.; Gwengo, C.; Lindeman, S. V.; Smith, M. D.; Long, G. J.; Grandjean, F.; Gardinier, J. R. *Inorg. Chem.* **2008**, *47*, 7233–7242.
(47) Marczenko, Z. *Spectroscopic Determination of the Elements*; Ellis Horwood Ltd.: Chichester, England, 1976.
(48) Rusanov, V.; Stankov, S.; Gushterov, V.; Tsankov, L.; Trautwein, A. X. *Hyperfine Interact.* **2006**, *169*, 1279.
(49) Winkler, H.; Chumakov, A. I.; Trautwein, A. X. *Top. Curr. Chem.* **2004**, *235*, 137.
(50) (a) *CRC Handbook of Chemistry and Physics*, 56th ed.; F-209; CRC Press: Boca Raton, FL. 1975; (b) Shannon, R. D. *Acta Crystallogr.* **1976**, *A32*, 751.